

## Supplementary Materials for

### Self-assembly of highly sensitive 3D magnetic field vector angular encoders

Christian Becker, Daniil Karnaushenko\*, Tong Kang, Dmitriy D. Karnaushenko, Maryam Faghieh,  
Alaleh Mirhajivarzaneh, Oliver G. Schmidt\*

\*Corresponding author. Email: d.karnaushenko@ifw-dresden.de (D.K.); o.schmidt@ifw-dresden.de (O.G.S.)

Published 20 December 2019, *Sci. Adv.* **5**, eaay7459 (2019)  
DOI: 10.1126/sciadv.aay7459

#### This PDF file includes:

Fig. S1. Characteristic of the  $ZY$  and  $XZ$  pairs (S1 and S3 and S5 and S6, respectively) of the orthogonal magnetic sensors formed on the opposite sides of the respective tube with the field rotating in the  $XY$  plane.

Fig. S2. Characteristic of the  $XY$  and  $XZ$  pairs (S2 and S4 and S5 and S6, respectively) of the orthogonal magnetic sensors formed on opposite sides of the respective tube with the field rotating in the  $ZY$  plane.

Fig. S3. Characteristic of the  $XY$  and  $ZY$  pairs (S2 and S4 and S1 and S3, respectively) of the orthogonal magnetic sensors formed on opposite sides of the respective tube with the field rotating in the  $XZ$  plane.

Fig. S4. Electrical breakdown of the sensors due to overheating under electrical stress.

Fig. S5. Mechanical reliability testing of encapsulated devices.

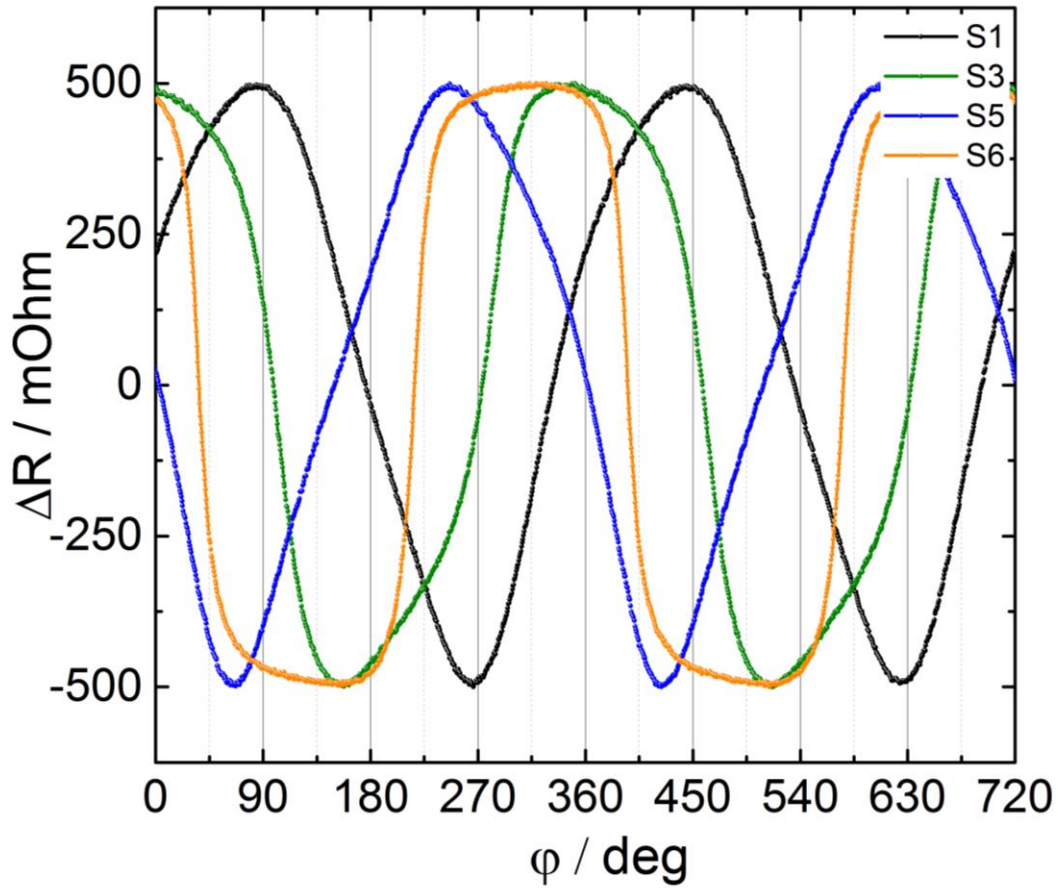


Fig. S1. Characteristic of the ZY and XZ pairs (S1 and S3 and S5 and S6, respectively) of the orthogonal magnetic sensors formed on the opposite sides of the respective tube with the field rotating in the XY plane.

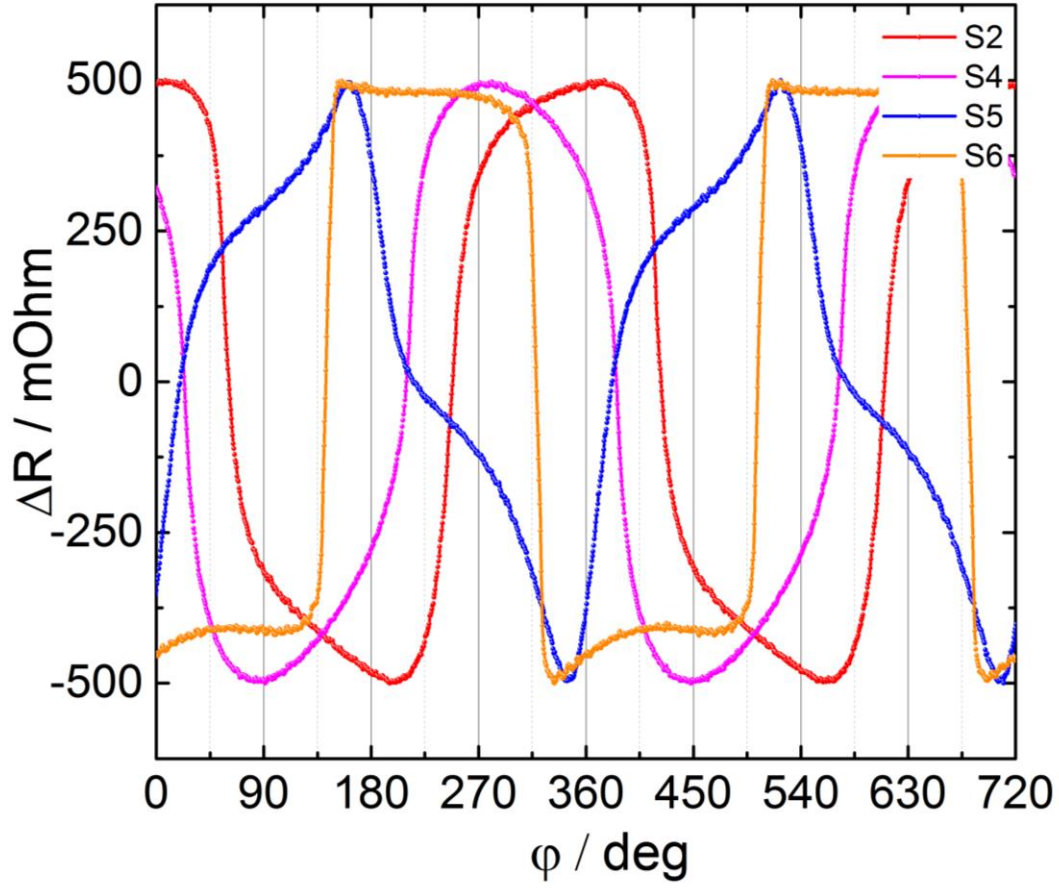


Fig. S2. Characteristic of the XY and XZ pairs (S2 and S4 and S5 and S6, respectively) of the orthogonal magnetic sensors formed on opposite sides of the respective tube with the field rotating in the ZY plane.

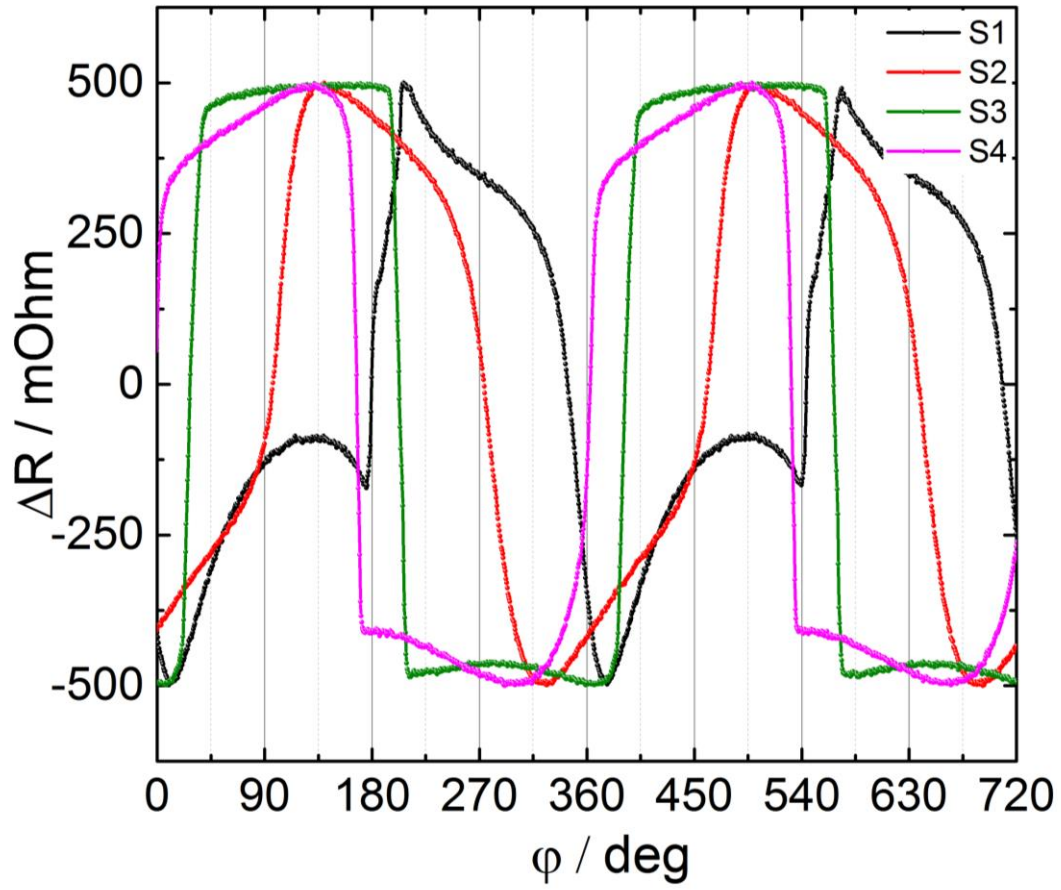
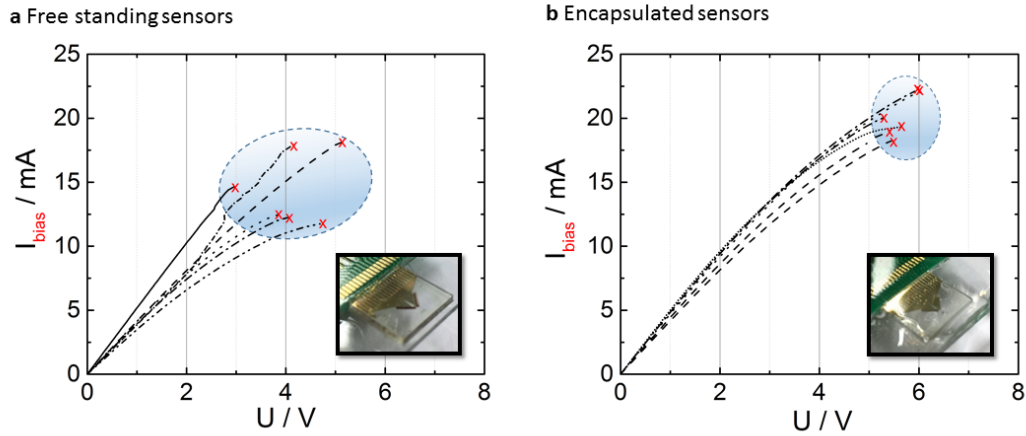
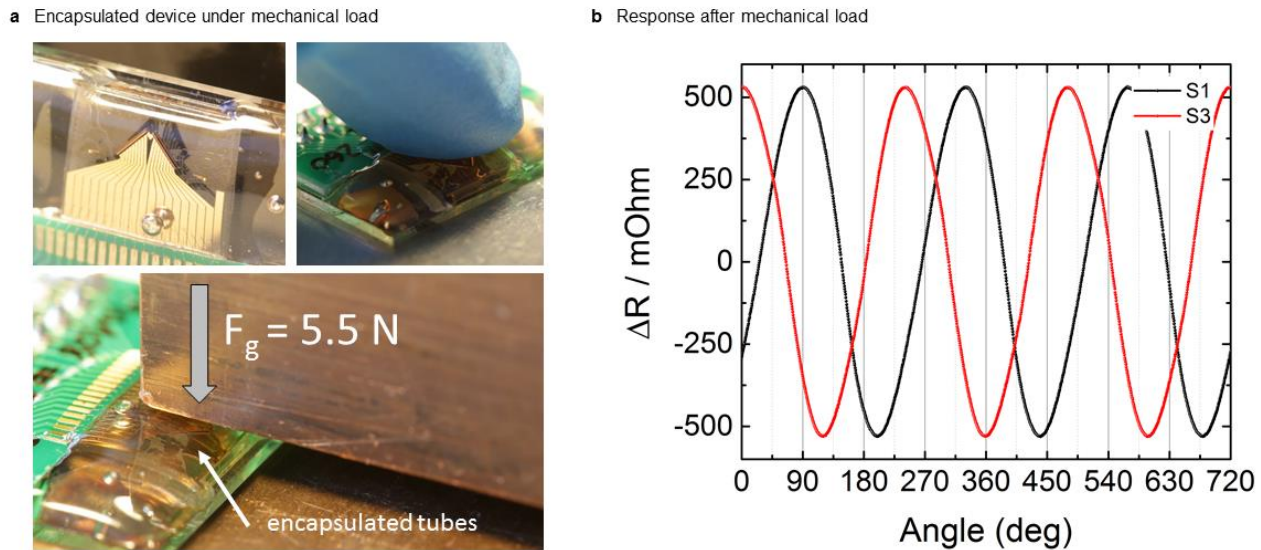


Fig. S3. Characteristic of the XY and ZY pairs (S2 and S4 and S1 and S3, respectively) of the orthogonal magnetic sensors formed on opposite sides of the respective tube with the field rotating in the XZ plane.



**Fig. S4. Electrical breakdown of the sensors due to overheating under electrical stress.** **a**, Breakdown of non-encapsulated sensors. **b**, Breakdown of encapsulated sensors. In both cases breakdown does not lead to mechanical deformation of the structure. Photos Credit: Christian Becker, Institute for Integrative Nanosciences Leibniz IFW Dresden.



**Fig. S5. Mechanical reliability testing of encapsulated devices.** **a**, Encapsulated device (top left panel) with a finger loading (top right panel) and loading with a defined mass (bottom panel) producing 5.5 N. **b**, Magnetoresistive-response of S1 and S3 to a rotating magnetic field after mechanical loadings indicating no negative effect on the sensor performance. Photos Credit: Christian Becker, Institute for Integrative Nanosciences Leibniz IFW Dresden.